Nonlinearity compensation in multi-rate 28 Gbaud WDM systems employing optical and digital techniques under diverse link configurations

Danish Rafique* **and Andrew D. Ellis**

Photonics Systems Group, Tyndall National Institute and Department of Electrical Engineering/Physics, University College Cork, Dyke Parade, Prospect Row, Cork, Ireland
**danish.rafique@tyndall.ie*

Abstract: Digital back-propagation (DBP) has recently been proposed for the comprehensive compensation of channel nonlinearities in optical communication systems. While DBP is attractive for its flexibility and performance, it poses significant challenges in terms of computational complexity. Alternatively, phase conjugation or spectral inversion has previously been employed to mitigate nonlinear fibre impairments. Though spectral inversion is relatively straightforward to implement in optical or electrical domain, it requires precise positioning and symmetrised link power profile in order to avail the full benefit. In this paper, we directly compare ideal and low-precision single-channel DBP with single-channel spectral-inversion both with and without symmetry correction via dispersive chirping. We demonstrate that for all the dispersion maps studied, spectral inversion approaches the performance of ideal DBP with 40 steps per span and exceeds the performance of electronic dispersion compensation by ~3.5 dB in *Q*-factor, enabling up to 96% reduction in complexity in terms of required DBP stages, relative to low precision one step per span based DBP. For maps where quasi-phase matching is a significant issue, spectral inversion significantly outperforms ideal DBP by ~3 dB.

OCIS codes: (060.2320) Fiber optics amplifiers and oscillators; (190.5040) Phase conjugation; (060.4370) Nonlinear optics, fibers.

References and links

1. A. D. Ellis, J. Zhao, and D. Cotter, "Approaching the non-linear Shannon limit," J. Lightwave Technol. **28**(4), 423–433 (2010).
2. X. Liu, S. Chandrasekhar, B. Zhu, P. J. Winzer, A. H. Gnauck, and D. W. Peckham, "448-Gb/s reduced-guard-interval CO-OFDM transmission over 2000 km of ultra-large-area fiber and five 80-GHz-grid ROADMs," J. Lightwave Technol. **29**(4), 483–490 (2011).
3. P. J. Winzer, A. H. Gnauck, S. Chandrasekhar, S. Draving, J. Evangelista, and B. Zhu, "Generation and 1,200-km transmission of 448-Gb/s ETDM 56-Gbaud PDM 16-QAM using a single I/Q modulator," European Conference on Optical Communications, PD2.2 (2010).
4. M. Nakazawa, S. Okamoto, T. Omiya, K. Kasai, and M. Yoshida, "256 QAM (64 Gbit/s) Coherent Optical Transmission over 160 km with an Optical Bandwidth of 5.4 GHz," Optical Fiber Communication Conference, OThD5 (2010).
5. D. Rafique and A. D. Ellis, "Nonlinear penalties in dynamic optical networks employing autonomous transponders," IEEE Photon. Technol. Lett. **23**(17), 1213–1215 (2011).
6. D. Rafique and A. D. Ellis, "Nonlinear penalties in long-haul optical networks employing dynamic transponders," Opt. Express **19**(10), 9044–9049 (2011).
7. A. Nag, M. Tornatore, and B. Mukherjee, "Optical network design with mixed line rates and multiple modulation formats," J. Lightwave Technol. **28**(4), 466–475 (2010).
8. C. Meusburger, D. A. Schupke, and A. Lord, "Optimizing the migration of channels with higher bitrates," J. Lightwave Technol. **28**(4), 608–615 (2010).
9. M. Suzuki, I. Morita, N. Edagawa, S. Yamamoto, H. Taga, and S. Akiba, "Reduction of Gordon-Haus timing jitter by periodic dispersion compensation in soliton transmission," Electron. Lett. **31**(23), 2027–2029 (1995).

#149559 - $15.00 USD Received 20 Jun 2011; revised 27 Jul 2011; accepted 8 Aug 2011; published 15 Aug 2011

10. D. D. Marcenac, D. Nesset, A. E. Kelly, M. Brierley, A. D. Ellis, D. G. Moodie, and C. W. Ford, "40 Gbit/s transmission over 406 km of NDSF using mid-span spectral inversion by four-wave-mixing in a 2 mm long semiconductor optical amplifier," Electron. Lett. **33**(10), 879–880 (1997).
11. I. Brener, B. Mikkelsen, K. Rottwitt, W. Burkett, G. Raybon, J. B. Stark, K. Parameswaran, M. H. Chou, M. M. Fejer, E. E. Chaban, R. Harel, D. L. Philen, and A. Kosinski, "Cancellation of all Kerr nonlinearities in long fiber spans using a LiNbO3 phase conjugator and Raman amplification," Optical Fiber Communication Conference, 266–PD33–1 (2000).
12. S. L. Jansen, D. Borne, B. Spinnler, S. Calabrò, H. Suche, P. M. Krummrich, W. Sohler, G. D. Khoe, and H. Waardt, "Optical phase conjugation for ultra long-haul phase-shift-keyed transmission," J. Lightwave Technol. **24**(1), 54–64 (2006).
13. F. M. Eduardo, Z. Xiang, and G. Li, "Electronic phase conjugation for nonlinearity compensation in fiber communication systems," Optical Fiber Communication Conference, JWA025 (2011).
14. P. Minzioni, I. Cristiani, V. Degiorgio, L. Marazzi, M. Martinelli, C. Langrock, and M. M. Fejer, "Experimental demonstration of nonlinearity and dispersion compensation in an embedded link by optical phase conjugation," IEEE Photon. Technol. Lett. **18**(9), 995–997 (2006).
15. G. Li, E. Mateo, and L. Zhu, "Compensation of nonlinear effects using digital coherent receivers," Optical Fiber Communication Conference, OWW1 (2011).
16. E. Ip, "Nonlinear compensation using backpropagation for polarization-multiplexed transmission," J. Lightwave Technol. **28**(6), 939–951 (2010).
17. D. Rafique, M. Mussolin, M. Forzati, J. Mårtensson, M. N. Chugtai, and A. D. Ellis, "Compensation of intra-channel nonlinear fibre impairments using simplified digital back-propagation algorithm," Opt. Express **19**(10), 9453–9460 (2011).
18. L. Lei, T. Zhenning, D. Liang, Y. Weizhen, O. Shoichiro, T. Takahito, H. Takeshi, and C. R. Jens, "Implementation efficient nonlinear equalizer based on correlated digital backpropagation," Optical Fiber Communication Conference, OWW3 (2011).
19. L. B. Du and A. J. Lowery, "Experimental demonstration of XPM compensation for CO-OFDM systems with periodic dispersion maps," Optical Fiber Communication Conference, OWW2 (2011).
20. M. Mussolin, D. Rafique, J. Mårtensson, M. Forzati, J. K. Fischer, L. Molle, M. Nölle, C. Schubert, and A. D. Ellis, "Polarization multiplexed 224 Gb/s 16QAM transmission employing digital back-propagation," European Conference on Optical Communications, accepted for publication (2011).
21. A. Chowdhury, G. Raybon, R. J. Essiambre, J. H. Sinsky, A. Adamiecki, J. Leuthold, C. R. Doerr, and S. Chandrasekhar, "Compensation of intrachannel nonlinearities in 40-Gb/s pseudolinear systems using optical-phase conjugation," J. Lightwave Technol. **23**(1), 172–177 (2005).
22. M. Shtaif and M. Eiselt, "Analysis of intensity interference caused by cross-phase modulation in dispersive optical fibers," IEEE Photon. Technol. Lett. **10**(7), 979–981 (1997).
23. S. J. Savory, G. Gavioli, R. I. Killey, and P. Bayvel, "Electronic compensation of chromatic dispersion using a digital coherent receiver," Opt. Express **15**(5), 2120–2126 (2007).
24. D. Rafique, J. Zhao, and A. D. Ellis, "Compensation of nonlinear fibre impairments in coherent systems employing spectrally efficient modulation format," IEICE Trans. Commun. **E94-B**(7), 1815–1822 (2011).
25. R. H. Stolen and C. Lin, "Self-phase-modulation in silica optical fibers," Phys. Rev. A **17**(4), 1448–1453 (1978).
26. A. Mecozzi, C. B. Clausen, and M. Shtaif, "Analysis of intrachannel nonlinear effects in highly dispersed optical pulse transmission," IEEE Photon. Technol. Lett. **12**(4), 392–394 (2000).
27. J. P. Gordon and L. F. Mollenauer, "Phase noise in photonic communications systems using linear amplifiers," Opt. Lett. **15**(23), 1351–1353 (1990).
28. D. Rafique and A. D. Ellis, "Impact of signal-ASE four-wave mixing on the effectiveness of digital back-propagation in 112 Gb/s PM-QPSK systems," Opt. Express **19**(4), 3449–3454 (2011).

1. Introduction

Recent trends in optical communication are focusing on high bit-rates as well as spectrally efficient transmission systems in order to cope with the demands of capacity growth [1]. Higher bit-rates per channel require the deployment of high-order modulation formats [2–5] with increased required optical signal-to-noise ratio (OSNR) and hence higher power per channel. Higher spectral efficiency also demands tightly spaced wavelength-division multiplexed (WDM) channels to maximize the utilization of the optical amplifier bandwidth. The ability to deploy a dynamic and configurable optical layer is a direct consequence of such developments. This is particularly true for shorter links across the network, where the improved optical signal-to-noise ratio (OSNR) would allow the use of a high capacity channel. While such dynamic multi-rate networks enable flexible capacity allocation, these systems present complex trade-offs. One such challenge is associated with the nonlinear transmission impairments [6], which strongly connect the achievable channel reach to a given modulation format and symbol-rate [5–8]. Historically, various methods of compensating fibre transmission impairments have been proposed, both in optical and electronic domain. Dispersion management was initially proposed to suppress the impact of fibre nonlinearity

#149559 - $15.00 USD Received 20 Jun 2011; revised 27 Jul 2011; accepted 8 Aug 2011; published 15 Aug 2011

[9]. Although this technique is beneficial, it enforces severe limitations on link design. Compensation of fibre impairments based on phase conjugation or spectral inversion (SI) was also proposed [10,11], however, although SI has large bandwidth capabilities, it necessitates precise positioning and symmetric link design (e.g., distributed Raman amplification, etc.). Whilst optical SI of WDM signals based on periodically poled lithium niobate waveguides has been demonstrated with negligible noise penalty and high conversion efficiency [12], electronic phase conjugation of a single channel has also been recently demonstrated based on intradyne detection [13]. Recently a modified SI approach has been proposed which exploits nonlinear temporal inversion by applying pre-compensation before the SI stage [14]. To mitigate some of the aforementioned drawbacks, electronic mitigation of nonlinear impairments using digital back-propagation (DBP) with time inversion has been applied to the compensation of channel nonlinearities [15,16]. However, despite its flexibility, the complexity of DBP is currently exorbitant due to ultra-wide bandwidth requirements (multi-channel DBP), significantly high number of required steps per link, and the requirement of prior knowledge of fibre span configuration, and therefore it still needs a considerable effort to make this method practically viable [17–19]. Recent efforts to simplify DBP [18] for PM-4QAM signals show up to 1.5 dB Q factor improvements in WDM transmission, although the benefit appears to reduce as the order of the modulation format is increased [20] and so for higher order modulation formats, we anticipate that a higher number of required steps per link will be required.

In this paper, we compare two single-channel nonlinearity compensation techniques: Digital back-propagation (ideal: high-precision and low-precision), and spectral inversion (non-symmetrised and symmetrised), for both dispersion compensating fibre (DCF) free and dispersion managed transmission links [21]. We report that spectral inversion approaches the performance of ideal DBP, and significantly outperforms linear compensation along with low-precision DBP. Furthermore, we demonstrate that for a dispersion map facilitating the suppression of fibre nonlinearity, SI outperforms even ideal high-precision DBP. To our knowledge, this is the first comparative report on the transmission performance of multi-precision digital back-propagation, and conventional and pre-chirped optical phase conjugation, employing multi-rate 28 Gbaud WDM transmissions with advanced modulation formats.

2. Principle of operation

In this section, we review the operating principle of the two forms of spectral inversion used in this paper: Standard SI (SSI) and pre-compensated SI (PSI). The SSI technique consists of the insertion of the SI device exactly at the midpoint of the link [11–13]. The PSI configuration described here is obtained starting from a SSI setup, and inserting a DCF before SI (pre-compensation) [14], as shown in Fig. 1. SI operation with WDM signals allows compensation of cross phase modulation (XPM) [22], however this adds to the networking constraints, and so in this paper we consider the use of single-channel SI only on those channels where self phase modulation (SPM) compensation is required.

PSI enables the use of SI in circumstances where the effective length (L_{eff}) is less than the amplifier spacing (L_{amp}) and the dispersion length is sufficiently small, thereby adding dispersion asymmetry. The effect of the added DCF is that of modifying the value of accumulated dispersion exhibited by the pulses during propagation along the nonlinear regions downstream of the SI. Note that an additional DCF must be inserted at the end of the link, or electronic compensation of additional dispersion can be applied [23]. We can see from Fig. 1 that for a conventional uncompensated map, the regions of high nonlinearity correspond to different accumulated dispersion on either side of SI, when SSI is employed. Whilst, the addition of a small piece of DCF applying compensation for (L_{amp}-L_{eff}) ensures that nonlinear effects occur for similar ranges of accumulated dispersion.

#149559 - $15.00 USD Received 20 Jun 2011; revised 27 Jul 2011; accepted 8 Aug 2011; published 15 Aug 2011

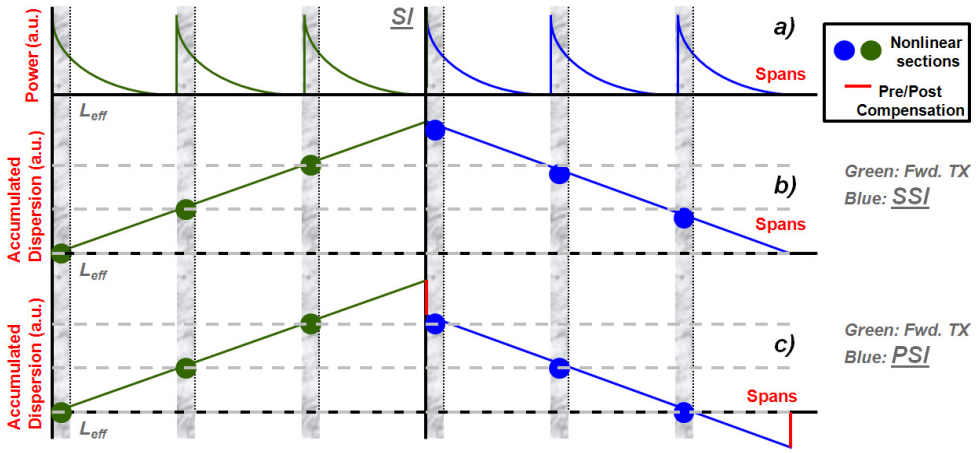

Fig. 1. Graphical representation for an uncompensated map showing, (a) Optical power profile, (b) Accumulated dispersion with SSI, and (c) Accumulated dispersion with PSI, as a function of number of spans. Solid circles represent regions of high nonlinearity.

3. Simulation setup

3.1 Transmitter

Figure 2 illustrates the simulation setup. The transmission system comprised nine 28 Gbaud WDM channels, employing PM-mQAM formats with a channel spacing of 50 GHz. A multi-rate system was employed with a 336 Gb/s central test-channel as PM-64QAM, and neighbouring 112 Gb/s channels as PM-4QAM channels. For all the carriers, both the polarization states were modulated independently using de-correlated 2^{15} and 2^{16} pseudo-random bit sequences (PRBS) with different random number seeds, for x- and y-polarization states, respectively. Each PRBS was de-multiplexed separately into two multi-level output symbol streams which were used to modulate an in-phase and a quadrature phase carrier. The optical transmitters consisted of continuous wave laser sources (5 kHz line-width), followed by two nested Mach-Zehnder Modulator structures for x- and y-polarization states, and the two polarization states were combined using an ideal polarization beam combiner. The simulation conditions ensured 16 samples per symbol with 2^{13} symbols per polarization (98,304 bits in total).

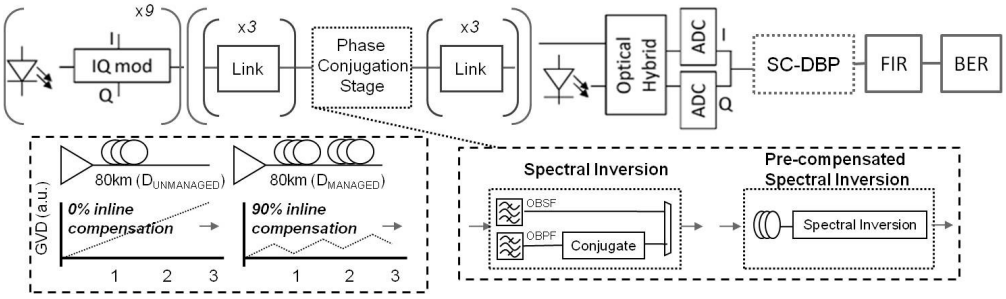

Fig. 2. Simulation setup for 28 Gbaud PM-mQAM (m = 4, 64) transmission system. Link: Dispersion profile as a function of number of spans for 0% and 90% inline dispersion compensation. Also, spectral inversion and pre-compensated spectral inversion architectures are shown.

#149559 - $15.00 USD Received 20 Jun 2011; revised 27 Jul 2011; accepted 8 Aug 2011; published 15 Aug 2011

3.2 Transmission link

The signals were multiplexed, and propagated over six 80 km spans for three fibre configurations with lumped erbium doped fibre amplification (EDFA), as shown in Fig. 2. Table 1 lists the relevant fibre parameters. We employed two transmission links with no inline dispersion compensation with either standard single-mode fibre (SSMF) or non-zero dispersion shifted fibre (NZDSF), and one short period dispersion managed link, specifically designed to suppress channel nonlinearities [21]. In the dispersion managed link 42 km of NZDSF was followed by 38 km of inverse NZDSF resulting in 18 ps/nm residual dispersion per span with near flat distribution of nonlinear regions. Single-stage EDFAs were used, where each amplifier stage was modelled with a 4.5 dB noise figure, and the total amplification gain was set to be equal to the total loss in each span.

Table 1. Fibre Types and Parameters

	$D_{UMMANAGED}$		$D_{MANAGED}$
Fibre Type/Parameters	SSMF	NZDSF	NZDSF(42km)-NZDSF(38km)
Dispersion (ps/nm/km)	20	4.5	0.22
Loss (dB/km)	0.2	0.2	0.2
Nonlinearity (1/W.km)	1.5	1.5	1.5
Dispersion Length, L_D (km)	~51	~245	~5000

3.3 Spectral inversion

In the middle of the link, the WDM signal is passed through a wavelength selective switch and the central 64QAM channel is spectrally inverted (see Fig. 2). In order to study the performance limits of the scheme, ideal SI is implemented by reversing the sign of the imaginary part of the signal. Note that optical [12] and electrical [13] implementations with sufficiently low penalties have already been reported. For PSI, a length of DCF equivalent to a dispersion of L_{amp}-L_{eff} of SSMF or NZDSF is applied (−1160 ps/nm and −261 ps/nm, respectively). The signal is then re-multiplexed with its unprocessed 4QAM neighbours. Note that PSI is not applied to the dispersion managed map since for this link $L_D >> L_{amp}$ ensuring that sufficient nonlinear symmetry is already present.

3.4 Receiver and digital back-propagation

At the coherent receiver the central PM-64QAM channel was de-multiplexed, pre-amplified, coherently-detected using four balanced detectors to give the baseband electrical signal and sampled at 2 samples per symbol. If SI was omitted, transmission impairments were digitally compensated via single-channel DBP (SC-DBP), which was numerically implemented by up-sampling the received signal to 16 samples/symbol and reconstructing the optical field from the in-phase and quadrature samples, followed by split-step Fourier method based solution of the nonlinear Schrödinger equation. Note that we considered a high number of samples per symbol to enable high DBP precision; however it has been shown previously that similar performance may be achieved with only 2 samples/symbol [24]. We employed multi-precision DBP where step-size was varied from 1 step per span to 40 steps per span (ideal). The performance with 2 steps per span here is close to that observed for the modified method of [17,18] with 1 step per span and is treated as a lower bound to low complexity. In context of recently proposed DBP simplification algorithms evaluated using a 4QAM baed system, the higher-order formats used here are more prone to fibre nonlinearity (high peak-to-average), necessitating higher numbers of required DBP steps to enable optimum performance [20]. Also, for comparison, electronic dispersion compensation (EDC) was employed using finite impulse response (FIR) filters (adapted using least mean square algorithm). In all cases, polarization de-multiplexing and residual dispersion compensation was performed using 13 tap FIR filters, followed by carrier phase recovery. Finally, the symbol decisions were made,

#149559 - $15.00 USD Received 20 Jun 2011; revised 27 Jul 2011; accepted 8 Aug 2011; published 15 Aug 2011

and the performance assessed by direct error counting (converted into an effective Q-factor (Q_{eff})). All the fibre propagations were carried out using VPItransmissionMaker®v8.5, and the digital signal processing was performed in MATLAB®7.10.

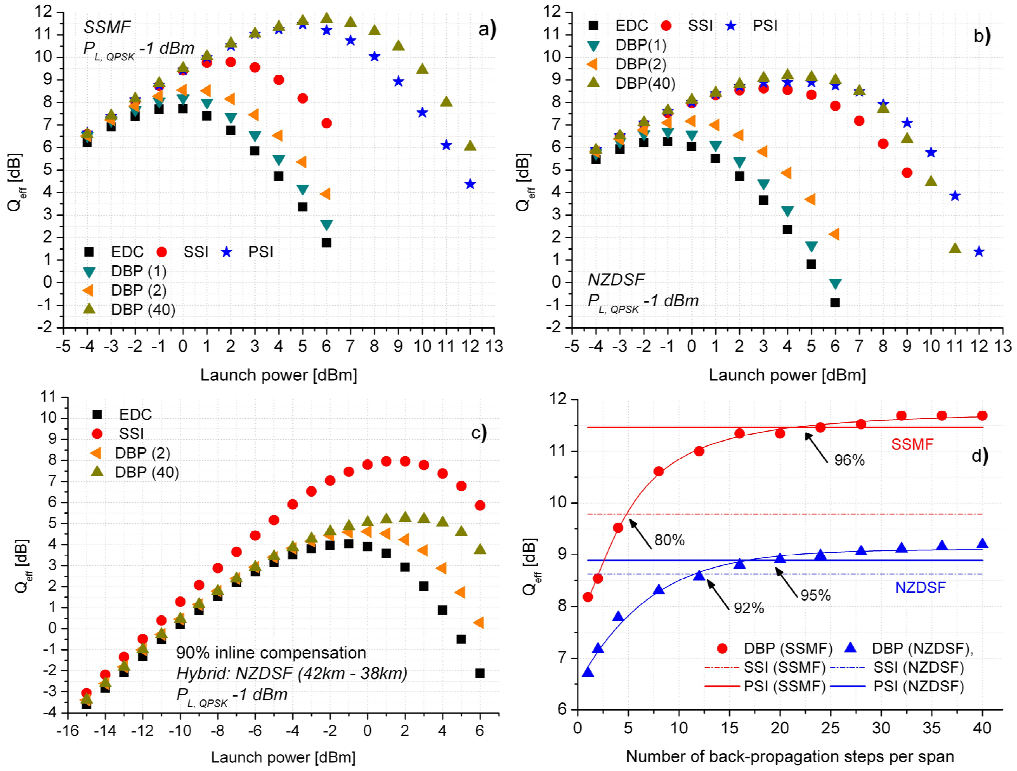

Fig. 3. Q_{eff} of central PM-64QAM channel as a function of launch power for various nonlinear compensation techniques. (a) SSMF with no inline dispersion compensation, (b) NZDSF with no inline dispersion compensation, (c) NZDSF with 90% inline dispersion compensation (hybrid transmission)., showing EDC (squares), SSI (circles), PSI (stars), DBP (1 step, down-triangle), DBP (2 steps, left-triangle), DBP (40 steps, up-triangle). (d) Q_{eff} as a function of number of back-propagation steps per span for SSMF (red) and NZDSF (blue) showing DBP (circles with solid fit), SSI (dotted line,) and PSI (thick solid line).

4. Results and discussions

Typical results of our simulations are shown in Fig. 3 as a function of signal launch power (P_L) for the central PM-64QAM channel. The launch power of all the neighbours was fixed at −1 dBm [5]. This is a practical approach for next-generation multi-rate networks, since OSNR requirements for low bit-rate channels are low; and hence lower launch power. This approach leads to reduced inter-channel nonlinearities, as demonstrated in [5], however the performance improvements enabled by single channel nonlinear compensation may vary depending on either homogenous [6] or heterogeneous [5] traffic is deployed. Figure 3 depicts the performance after EDC, SSI, PSI and DBP. At lower launch powers, the system is noise-limited and Q_{eff} of all approaches overlap. As we increase the launch power, nonlinear effects become significant and the different approaches demonstrate different optimum launch power, reflecting their dissimilar nonlinear compensation effects. Figure 4 qualitatively depicts the difference in performance between SI (top) and EDC (bottom) at the optimum launch power, for various dispersion maps studied in Fig. 3.

#149559 - $15.00 USD Received 20 Jun 2011; revised 27 Jul 2011; accepted 8 Aug 2011; published 15 Aug 2011

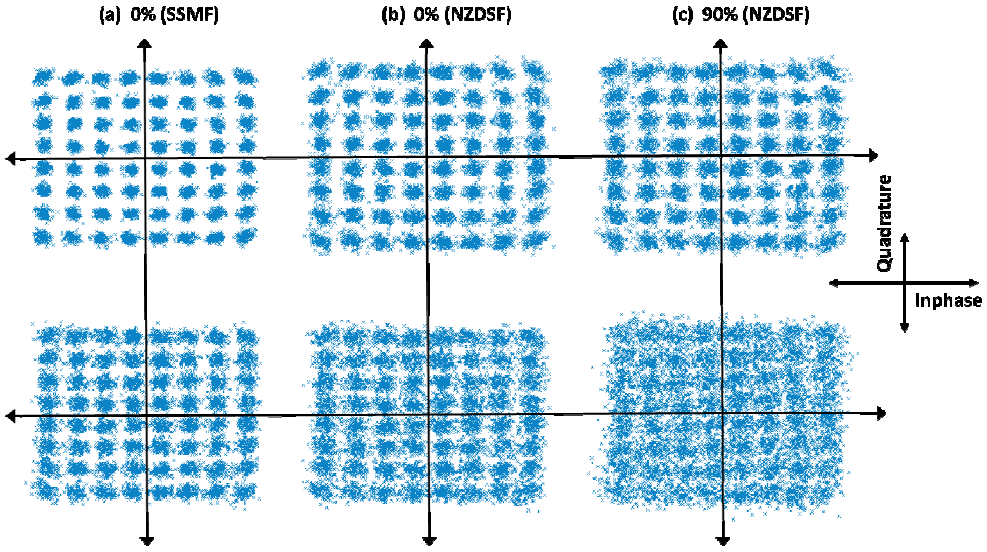

Fig. 4. Constellation maps after SI (top) and EDC (bottom) for 28 Gbaud PM-64QAM at optimum launch power. (a) 0% inline compensation (SSMF), PSI and EDC (b) 0% inline compensation (NZDSF), PSI and EDC (c) 90% inline compensation (NZDSF), SSI and EDC.

As expected for all the fibre configurations in Fig. 3, full precision DBP and both forms of SI outperform EDC, and for these configurations all of the studied reduced complexity DBP; also outperform EDC. For the uncompensated links (Fig. 3(a) and Fig. 3(b)), enhancing the accuracy of SI by employing pre-compensated SI (PSI) enables the performance of DBP(40) to be approached. In the case of SSMF (Fig. 3(a)), the remaining compensation asymmetry, due to inherent first-order approximation of nonlinear impairments taking place within L_{eff}, results in a slight penalty of ~0.3 dB. This penalty is almost completely eliminated for low dispersion fibres (L_D>L_{amp}). For the dispersion managed transmission (Fig. 3(c)), the symmetry of the nonlinear regions is sufficient for the uncompensated standard SI (SSI) to even outperform all forms of electronic compensation. Note that in this study, we have assumed a dynamic network where each channel operates at its minimum power, and so the primary limitation arises from intra-channel nonlinearities, such as self-phase modulation [25] and intra-channel four-wave mixing (L_D<<L_{eff}) [26], Gordon-Mollenauer (L_D>>L_{amp}) [27] and parametric noise amplification (all the dispersion lengths) [28]. Whilst self-phase modulation and intra-channel four-wave mixing are ideally compensated in all the dispersion regimes, the remaining two involve a nonlinear interaction with noise which is only partially compensable. In the case fo DBP, these effects both favour the highest possible local dispersion (lowest L_D). However, due to the dependence of the compensation accuracy of PSI on waveform symmetry, PSI favours low dispersion (high L_D), and so presents a clear trade-off between compensation accuracy and intra-channel nonlinearity. This results in marginally improved performance with ideal DBP for the highest dispersion fibre, but slightly greater performance for PSI uncompensated NZDSF.

In the case of dispersion managed fibre, the compensation symmetry ($(L_{amp}$-$L_{eff})/L_D$) is sufficiently high to enable the use of SSI, but the low dispersion also exacerbates the impact of parametric noise amplification. In this case, parametric noise amplification demonstrates super-linear length dependence, and splitting the link into two halves results in a significant reduction in the impact of this effect, enabling SSI to outperform ideal DBP significantly. A corollary of these results is that we would expect PSI to begin to outperform DBP for longer transmission distances.

#149559 - $15.00 USD Received 20 Jun 2011; revised 27 Jul 2011; accepted 8 Aug 2011; published 15 Aug 2011

Having established that PSI matches, or outperforms 40 steps per span DBP, it remains to analyse the implementation complexity and power consumption of two techniques. Figure 3(d) shows the performance of DBP with varying precision or step size per span, both for SSMF and NZDSF. It can be seen that for SSMF, SSI and PSI enable performance improvements equivalent to DBP employing ~5 steps per span and ~22 steps per span, respectively. This can be seen as SSI and PSI enabling 80% and 96% simplifications to one step per span SC-DBP. Likewise, for low dispersion fibre, SSI and PSI enable performance enhancements corresponding to 12 steps per span and 18 steps per span, respectively. These findings clearly demonstrate that even though significant efforts are put into simplifying standard DBP algorithms, conventional simplistic SI radically outperforms DBP technique. However, these considerable savings in application specific integrated circuit (ASIC) complexity and computational load must of course be traded-off with the complexity of adding PSI at appropriate network node, suggesting that a hybrid solution using SI to compensate the bulk of the SPM, and simplified DBP to accommodate the residual penalties due to varying SI location would offer the optimum configuration.

5. Conclusion

We have compared various nonlinearity compensation techniques and have reported that single-channel spectral inversion always outperforms low-precision single-channel digital back-propagation. We have also demonstrated that the performance of SI is further increased by employing pre-chirped SI, approaching the performance of ideal 40 steps per span DBP. Our results suggest that employing SI at ROADM site would significantly reduce the DBP computational load, leading to an optimum hybrid solution to compensate fibre nonlinearity. In particular, compared to single-step per span DBP, symmetrised SI enables Q_{eff} improvement up to ~3.5 dB and P_L improvement up to ~6 dB, equivalent to ideal SC-DBP, in a coherently-detected mixed bit-rate 28 Gbaud PM-mQAM WDM system. Furthermore, for some legacy dispersion managed links SI may enable enhanced performance that DBP. Note that for networks employing homogenous traffic, the complexity reductions reported here will remain valid, however with reduced intra-channel nonlinearity compensation benefits due to strong cross-phase modulation effects.

Acknowledgments

This work is supported by Science Foundation Ireland and CTVR II under Grant 06/IN/I969 and 10/CE/I1853, respectively.

#149559 - $15.00 USD Received 20 Jun 2011; revised 27 Jul 2011; accepted 8 Aug 2011; published 15 Aug 2011